Обзор ArXiv/astro-ph, 2-10 марта 2022

От Сильченко О.К.

ArXiv: 2203.00689

Kiloparsec view of a typical star-forming galaxy when the Universe was ~ 1 Gyr old

II. Regular rotating disk and evidence for baryon dominance on galactic scales

R. Herrera-Camus[1], N. M. Förster Schreiber[2], S. H. Price[2], H. Übler[3,4], A. D. Bolatto[5], R. L. Davies[6,7], D. Fisher[6,7], R. Genzel[2], D. Lutz[2], T. Naab[8], A. Nestor[9], T. Shimizu[2], A. Sternberg[2,9,10], L. Tacconi[2], and K. Tadaki[11]

[1] Departamento de Astronomía, Universidad de Concepción, Barrio Universitario, Concepción, Chile
e-mail: rhc@astro-udec.cl
[2] Max-Planck-Institut für extraterrestische Physik (MPE), Giessenbachstr., D-85748 Garching, Germany
[3] Cavendish Laboratory, University of Cambridge, 19 J.J. Thomson Avenue, Cambridge CB3 0HE, UK
[4] Kavli Institute for Cosmology, University of Cambridge, Madingley Road, Cambridge CB3 0HA, UK
[5] Department of Astronomy, University of Maryland, College Park, MD 20742, USA
[6] Centre for Astrophysics and Supercomputing, Swinburne Univ. of Technology, P.O. Box 218, Hawthorn, VIC 3122, Australia
[7] ARC Centre of Excellence for All Sky Astrophysics in 3 Dimensions (ASTRO 3D), Australia
[8] Max-Planck Institute for Astrophysics, Karl Schwarzschildstrasse 1, D-85748 Garching, Germany
[9] School of Physics and Astronomy, Tel Aviv University, Ramat Aviv 69978, Israel
[10] Center for Computational Astrophysics, 162 5th Ave., New York, NY, 10010
[11] National Astronomical Observatory of Japan, 2-21-1 Osawa, Mitaka, Tokyo 181-8588, Japan

Received ; accepted

Paper 1: HZ4, ALPINE

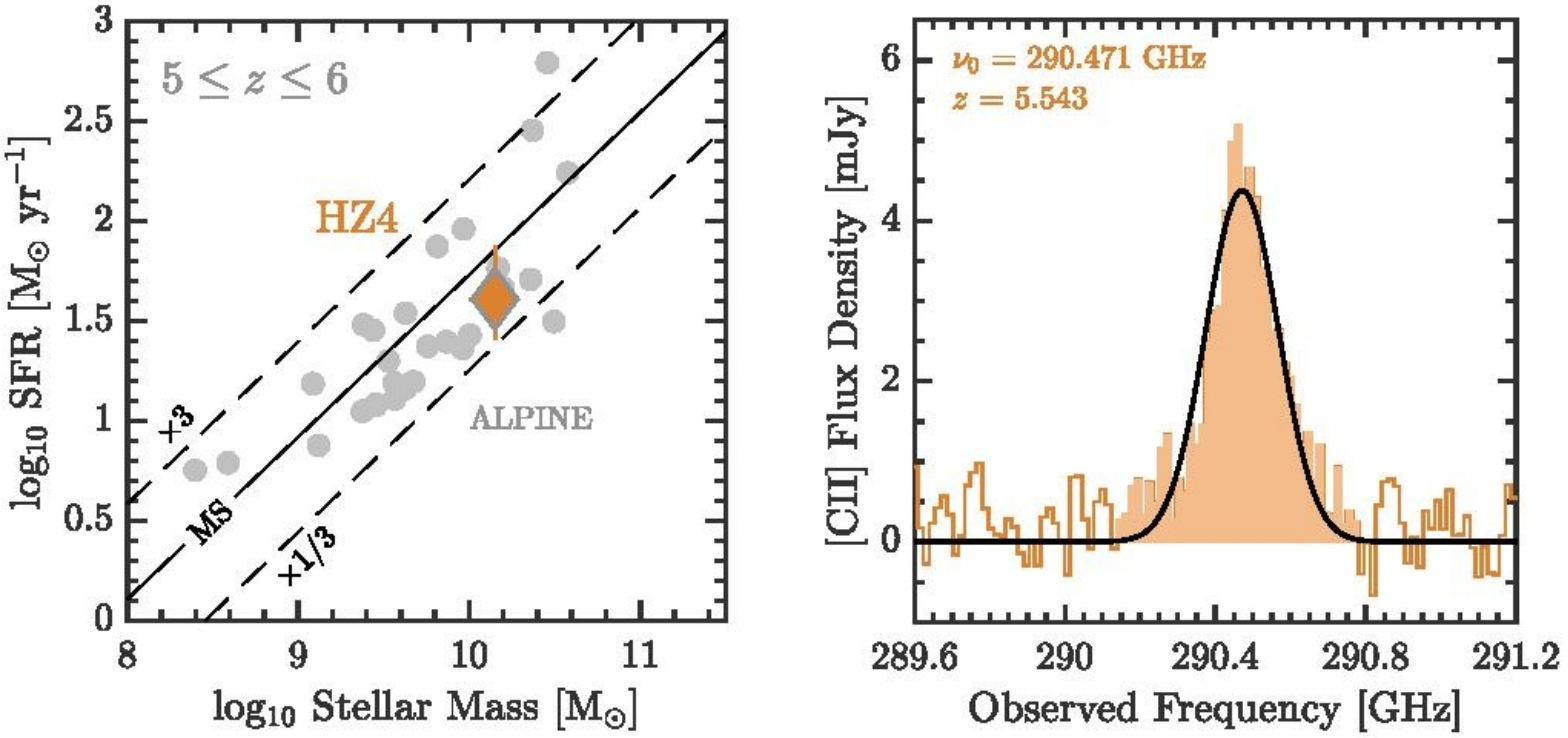

Fig. 1. *Left*: star formation rate – stellar mass plane between $5 \leq z \leq 6$ showing the position of the main sequence of star-forming galaxies (black line; Speagle et al. 2014) and the $z \sim 5$ galaxies with [C II] detections in the ALPINE survey (gray circles; Le Fèvre et al. 2020; Faisst et al. 2020). HZ4, shown as an orange diamond, lies only ~0.2 dex above the main sequence and can be considered a typical star-forming galaxy at this redshift (Faisst et al. 2020). *Right*: continuum-subtracted [C II] 158 μm spectrum of HZ4 extracted inside a circular aperture of 0.9″ radius (~5.4 kpc). The best Gaussian fit is centered at an observed frequency of $\nu_0 = 290.471$ GHz, which corresponds to a redshift of $z = 5.54$.

Разрешаются изображения: и в линии газа, и в пыли, и в УФ/HST

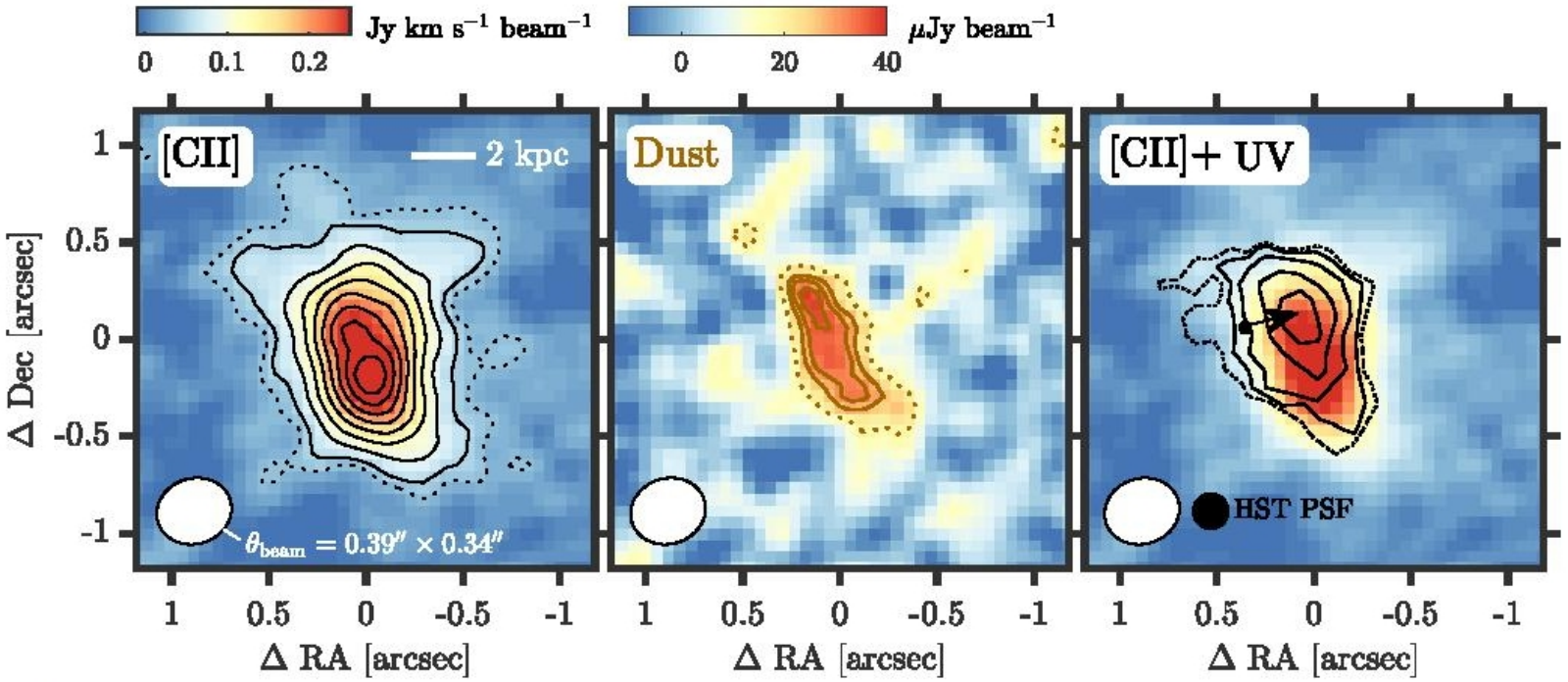

Fig. 2. *Left*: [C II] 158 μm integrated intensity of HZ4. The contours start at 2σ (dotted line) and then increase from 3σ to 17σ in steps of two (solid lines). The ALMA-synthesized beam ($\theta = 0.39'' \times 0.34''$) is shown in the bottom left corner. *Center*: dust continuum emission at rest-frame 160 μm. The contours level are 2 (dotted brown line), and 3, 3.5, and 4σ (solid brown lines). *Right*: contours of rest-frame UV emission as observed by HST WFC3 *F*160*W* (Barisic et al. 2017) overlaid on the [C II] integrated intensity map. The contour levels are 2 (dashed black line), 3, 5, 10, and 20σ (solid black lines). The contours are shifted in the direction of the black arrow from the original position marked by the black dot. The HST WFC3 *F*160*W* point-spread function is shown in black in the bottom left corner next to the ALMA beam in white.

Морфологически – большой диск

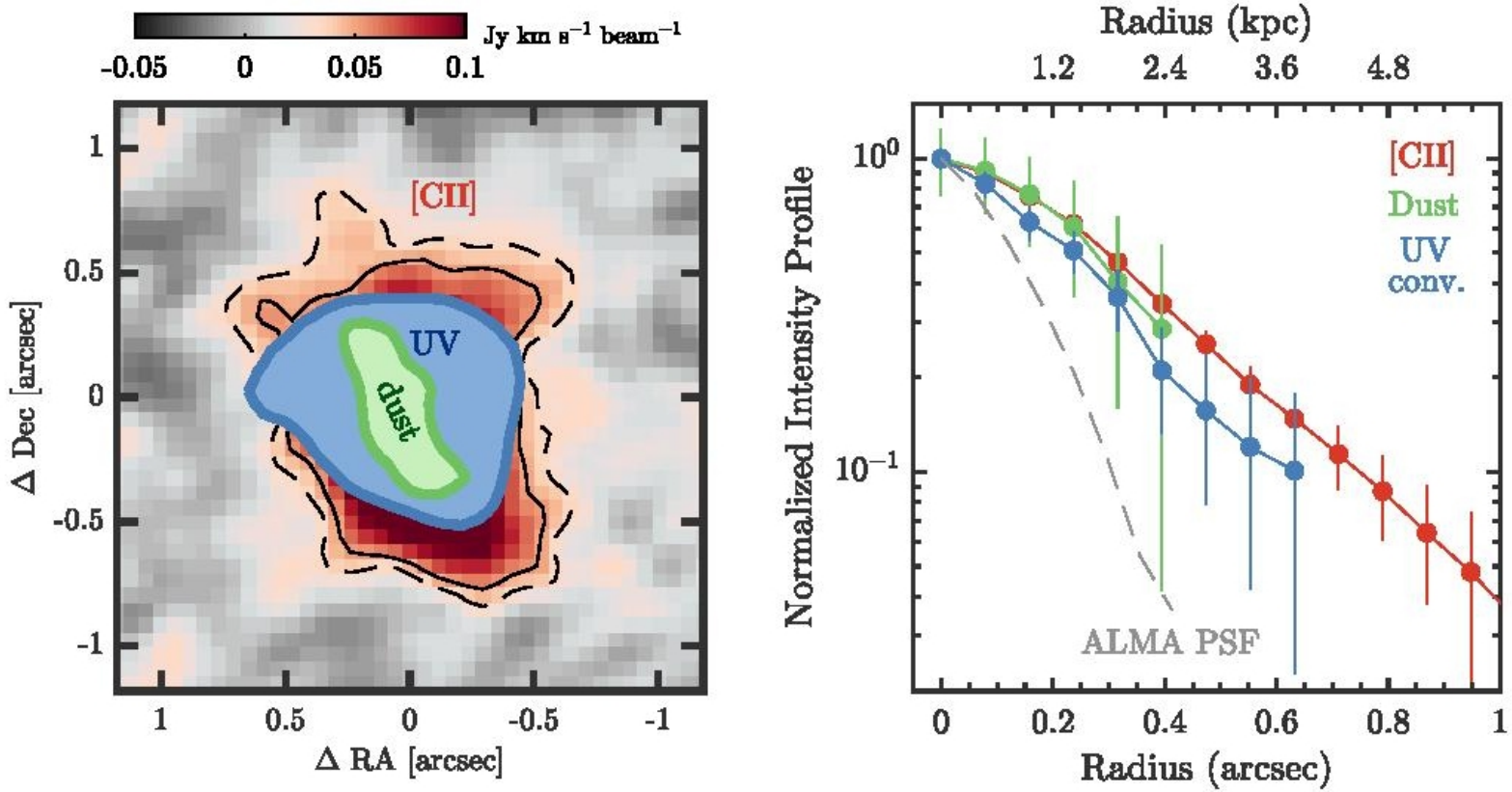

Fig. 7. *Left*: integrated intensity map of the [C II] line emission. The extent of the dust and convolved rest-frame UV continuum emission with $S/N > 3$ is shown in green and blue, respectively. *Right*: normalized radial intensity profile for the [C II] line (red), dust continuum (green), and convolved rest-frame UV continuum emission (blue). The common ALMA beam intensity profile is shown with a dashed gray line. The distance from the center is shown in arcseconds (bottom) and projected kiloparsec (top, not corrected for inclination).

Paper 2: Поле скоростей

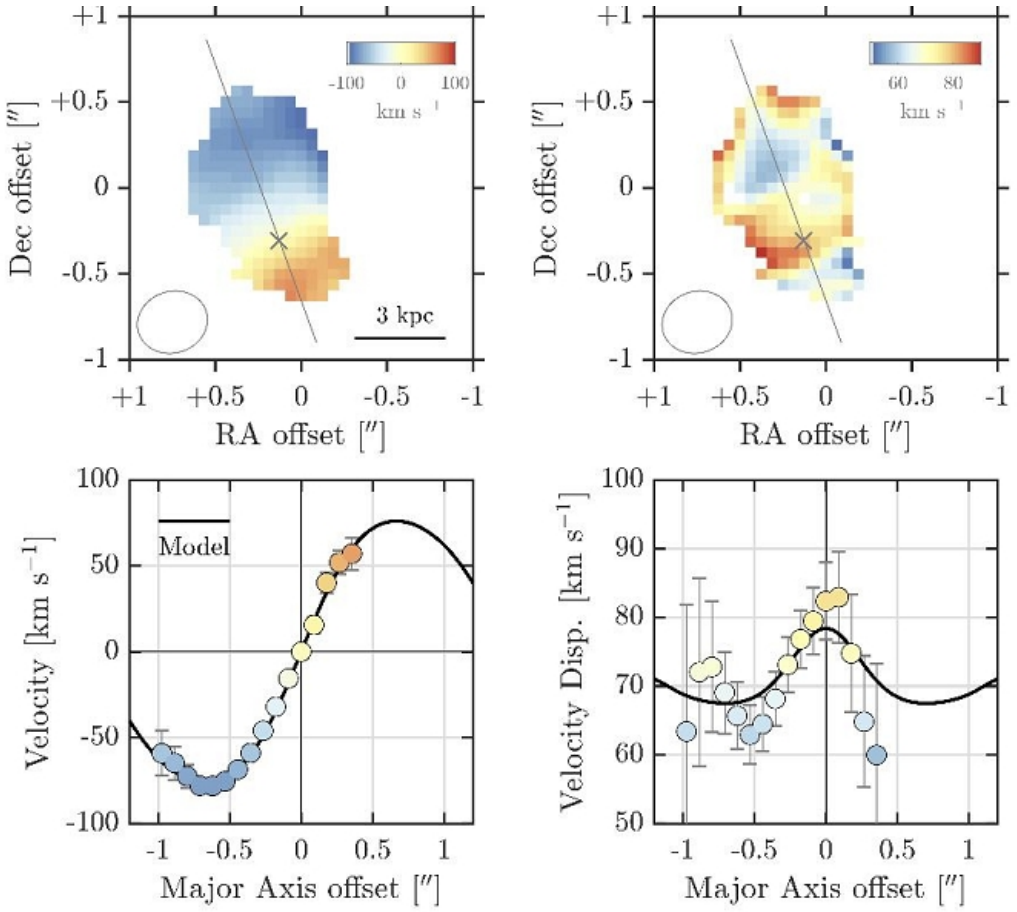

Fig. 1. *(Top)* [C II] velocity field (left) and velocity dispersion map (right) of HZ4. The ALMA synthesized beam ($\theta = 0.39'' \times 0.34''$) is shown in the bottom-left corner. *(Bottom)* Rotation curve and velocity dispersion profiles extracted employing a pseudo-slit oriented along the kinematic major axis shown by the gray solid line in the upper panels, where the kinematic center is shown with a gray cross. The solid black line in both panels represent the best-fit DYSMAL model beam-convolved to the observed space.

Диск горячеват, но все же поддерживается вращением

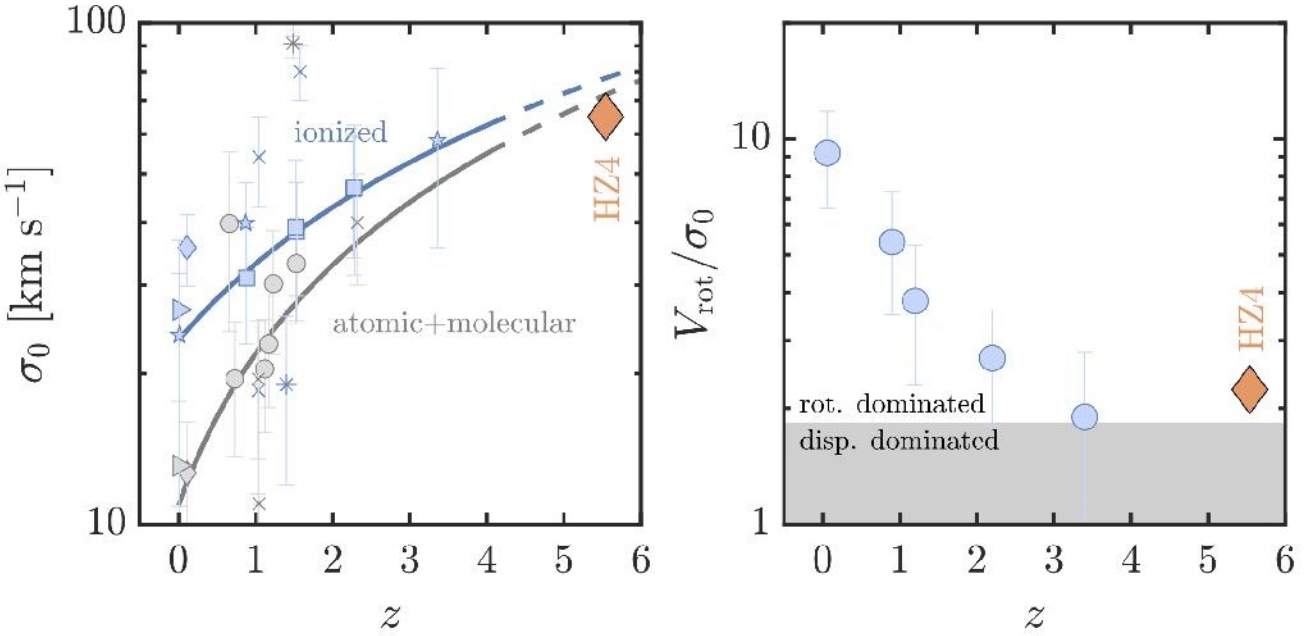

Fig. 2. Evolution of the intrinsic velocity dispersion (σ_0; left) and the disk dynamical support ($V_{\rm rot}/\sigma_0$; right) as a function of redshift. HZ4 at $z \approx 5$ is shown as an orange diamond. In the left panel, the circles show average values from different surveys of ionized (blue) and atomic and/or molecular gas (gray). These include: DYNAMO (diamonds; Fisher et al. 2019; Girard et al. 2021), HERACLES, THINGS and EDGE (triangles; Leroy et al. 2008, 2009; Mogotsi et al. 2016; Bolatto et al. 2017a,b), KMOS^{3D} and SINS/zC-SINF (squares; Förster Schreiber et al. 2006, 2009; Wisnioski et al. 2015, 2019; Übler et al. 2019), PHIBSS (circles; Tacconi et al. 2013; Freundlich et al. 2019), and GHASP/KDS/KROSS (stars; Epinat et al. 2010; Stott et al. 2016; Turner et al. 2017; Johnson et al. 2018). We also add individual measurements from lensed systems (crosses) from Swinbank et al. (2011) and Girard et al. (2019), and unlensed systems (asterisks) from Molina et al. (2019) and Übler et al. (2018). The solid lines show the best-fit relations to the observations compiled by Übler et al. (2019) up to $z \approx 3.5$. In the right panel, the circles show the average values for $V_{\rm rot}/\sigma_0$ from the ionized gas measured and compiled by Wisnioski et al. (2015). The gray box shows the region below $V_{\rm rot}/\sigma_0 = \sqrt{3.36}$ where the contribution to the dynamical support of the disk by random motions starts to dominate (e.g., Förster Schreiber & Wuyts 2020).

В области измеренного поля скоростей доминируют барионы

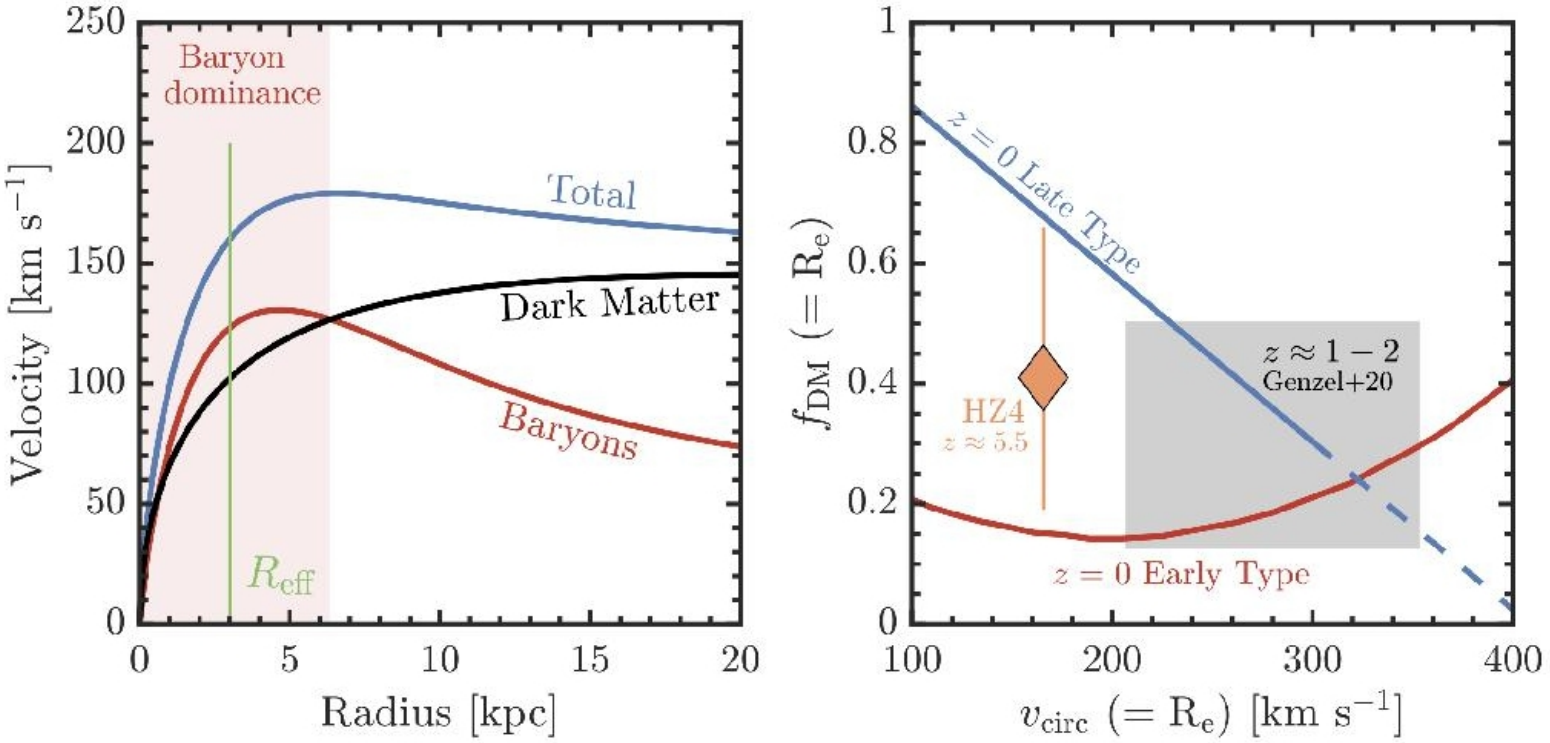

Fig. 3. (*Left*) Intrinsic rotation curve (corrected by inclination) of HZ4 for baryons (red), dark matter (black), and total (blue) from the best-fit model. The green vertical line shows the R_e, and the red colored box represents the spatial scales of baryon dominance in HZ4. (*Right*) Dark matter fraction within R_e of HZ4 (orange diamond), main-sequence, star-forming galaxies at $z \approx 1-2$ (gray box; Genzel et al. 2020), and the best linear fit to $z \sim 0$ late type galaxies (blue line), and $z \sim 0$ ATLAS-3D early type galaxies (red curve; Cappellari 2016).

Турбулентность соответствует темпам звездообразования

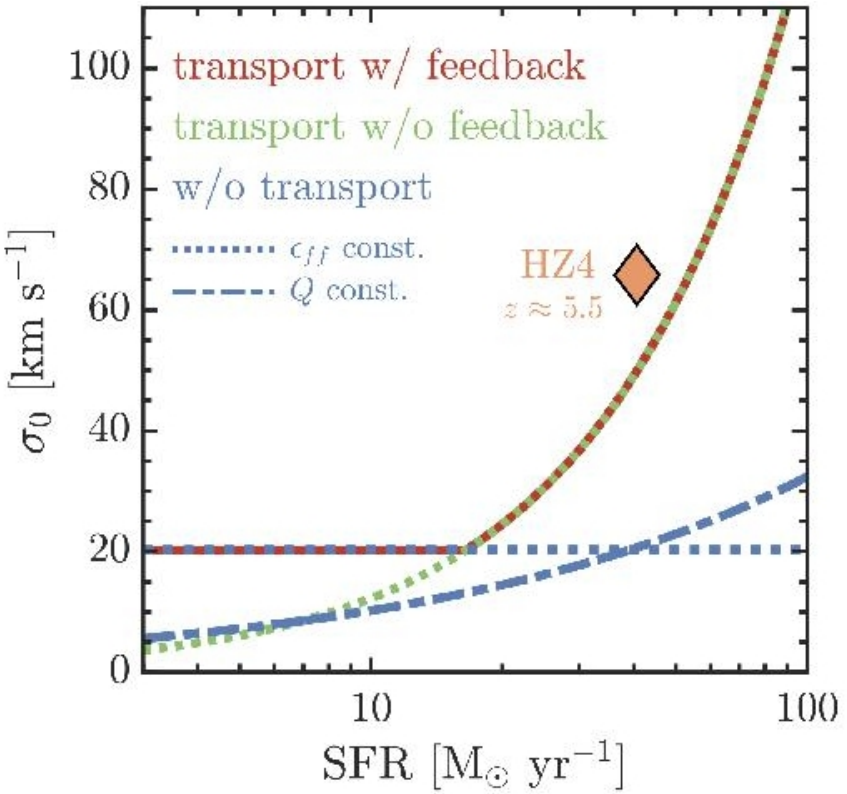

Fig. 4. Intrinsic velocity dispersion σ_0 as a function of star formation rate SFR for HZ4 (orange diamond), and the unified models by Krumholz et al. (2018) for high-z galaxies that consider transport+feedback (red), only transport (green), and feedback without transport (blue): the dotted and dashed lines correspond to the models with constant $\epsilon_{\rm ff}$ and constant Q, respectively.